

# Carpal kinematics in quadrupedal monkeys: towards a better understanding of wrist morphology and function

Guillaume Daver<sup>1</sup>, Gilles Berillon<sup>2</sup> and Dominique Grimaud-Hervé<sup>1</sup>

<sup>1</sup>Département de Préhistoire, UMR 7194 Muséum National d'Histoire Naturelle, Paris, France

<sup>2</sup>UPR 2147 CNRS, Paris, France

## Abstract

The purpose of this study is to provide new data on carpal kinematics in primates in order to deepen our understanding of the relationships between wrist morphology and function. To that end, we provide preliminary data on carpal kinematics in seven species of quadrupedal monkeys that have not been previously investigated in this regard (cercopithecoids,  $n = 4$ ; ceboids,  $n = 3$ ). We radiographed wrists from cadavers at their maximum radial and ulnar deviations, as well as at maximum flexion and extension. We took angular measurements to quantify the contribution of the mobility of the two main wrist joints (antebrachiocarpal and midcarpal) with respect to total wrist mobility. We also recorded qualitative observations. Our quantitative results show few clear differences among quadrupedal monkeys for radioulnar deviation and flexion–extension: all the primates studied exhibit a greater midcarpal mobility (approximately 54–83% of the total range of motion) than antebrachiocarpal mobility; however, we identified two patterns of carpal kinematics that show the functional impact of previously recognised morphological variations in quadrupedal monkeys. Firstly, qualitative results show that the partition that divides the proximal joint of the wrist in ceboids results in less mobility and more stability of the ulnar part of the wrist than is seen in cercopithecoids. Secondly, we show that the olive baboon specimen (*Papio anubis*) is characterised by limited antebrachiocarpal mobility for extension; this effect is likely the result of a radial process that projects on the scaphoid notch, as well as an intraarticular meniscus. Because of these close relationships between carpal kinematics and morphology in quadrupedal monkeys, we hypothesise that, to some extent, these functional tendencies are related to their locomotor hand postures.

**Key words:** comparative anatomy; functional morphology; hand postures; locomotion; radiography; wrist joints.

## Introduction

The relationship between wrist morphology and its function in primates is a long-standing subject of inquiry (e.g. Napier, 1962, 1967, 1980; Lewis, 1965, 1969, 1971a,b, 1974, 1985, 1989; Tuttle, 1967, 1969; Sarmiento, 1988; Hamrick, 1996). This issue results from the morphological complexity of the wrist, which involves numerous bones and ligaments (Sarmiento, 1988; Lewis, 1989). Hence, any functional interpretations of the morphological variation of the primate wrist must rely on accurate descriptions of carpal bone movements (or carpal kinematics) in their anatomical context (Jenkins, 1981). Previous analyses of carpal kinematics

in primates initially focused on apes because of their close phylogenetic relationships with humans (Schreiber, 1934; Yalden, 1972; Jenkins & Fleagle, 1975; O'Connor & Rarey, 1979; Jenkins, 1981; Jouffroy & Medina, 2002; Orr et al. 2010); however, kinematic data pertaining to monkeys are largely lacking in the literature. The purpose of this study is to provide new data on carpal kinematics of monkeys (ceboids and cercopithecoids) that have not been previously investigated in order to first develop a suitable comparative framework for studies of the functional morphology of the wrist of quadrupedal monkeys; and second to deepen our understanding of the relationships between wrist morphology and its associated functions.

Monkeys are primarily quadrupedal primates (Rose, 1973; Fleagle, 1999), and they use at least five types of locomotor hand postures: palmigrady; graspwalk; schizodactyl graspwalk; clawed quadrupedalism; and digitigrady (Hunt et al. 1996); however, digitigrady differs from other hand postures because of the absence of contact between the

### Correspondence

Guillaume Daver, Département de Préhistoire, UMR 7194  
Muséum National d'Histoire Naturelle, Paris, France.  
E: daver@mnhn.fr

Accepted for publication 6 October 2011  
Article published online 4 November 2011

palm and the support during the stance phase (Whitehead, 1993; Patel, 2009, 2010; Patel & Polk, 2010). This hand posture is associated with limited wrist mobility in extension and ulnar deviation (Schreiber, 1934; Sullivan, 1961; Jones, 1967; Tuttle, 1969; Lemelin & Schmitt, 1998; Richmond, 2006). Digitigrady is used habitually by terrestrial cercopithecine monkeys, including baboons (*Papio*), geladas (*Theropithecus*), mandrills (*Mandrillus*), patas monkeys (*Erythrocebus*) and, occasionally, semiterrestrial species such as macaques (*Macaca*), vervet monkeys (*Chlorocebus*) mangabeys (*Cercocebus*) and possibly some guenons (e.g. *Cercopithecus*, *Allenopithecus*; Bishop, 1964; Napier & Napier, 1967; Tuttle, 1969; Rose, 1973, 1977; Kingdon, 1988; Rawlins, 1993; Whitehead, 1993; Gautier-Hion et al. 1999; Chatani, 2003; Patel, 2009, 2010). Therefore, quadrupedal monkeys use different substrates and hand postures, and these differences should involve variations in carpal kinematics.

Comparative studies of monkey wrists have attempted to highlight relationships between morphology and carpal kinematics (e.g. Jones, 1967; Yalden, 1972; Ziemer, 1978; Fleagle & Meldrum, 1988; Lewis, 1989; Youlatos, 1996; Lemelin & Schmitt, 1998; Schwartz & Yamada, 1998; Patel & Carlson, 2006; Richmond, 2006). The wrists of quadrupedal monkeys are composed of nine carpal bones organised in two rows (a proximal and a distal row), and two main joints (a proximal or antebrachio-carpal joint and a distal or mid-carpal joint; Fig. 1). Digitigrade monkeys share a radial dorsal process that projects into a depression on the scaphoid as well as a meniscus interposed between the dorsal parts of the radius and scaphoid. These morphological traits are absent in non-digitigrade monkeys and are assumed to be associated with a limited extension of the proximal carpal row (Jones, 1967; Yalden, 1972; Lewis, 1989; Fig. 1). In addition, the lunate articular surface on the radius in digitigrade monkeys is particularly dense in the dorsal region, whereas it is dense over the entire surface in other monkeys; that trait is assumed to be associated with a maximum congruence of the radius-lunate joint in extension (Carlson & Patel, 2006; Patel & Carlson, 2006). In addition, the articular surfaces of the capitate-hamate complex are proximally flattened and would limit the amplitudes of radioulnar deviation at the midcarpal joint in cercopithecoids (Lemelin & Schmitt, 1998; Fig. 1). In contrast, most quadrupedal ceboids are characterised by the retention of a primitive trait shared by other mammals: a partition called the synovial septum that divides the joint between the forearm and the wrist into two compartments (Cartmill & Milton, 1977). This septum distally links the lunate-triquetrum ligament to the proximal ligament that unites the distal parts of the radius and the ulna. This septum is absent or vestigial in the capuchin monkey (*Cebus*), the red-faced spider monkey (*Ateles*), the woolly monkey (*Lagothrix*) and Old World monkeys (cercopithecoids; Parsons, 1900; Beattie, 1927; Robertson, 1944; Hill, 1957, 1959, 1960, 1962, 1966, 1970, 1974; Lewis,

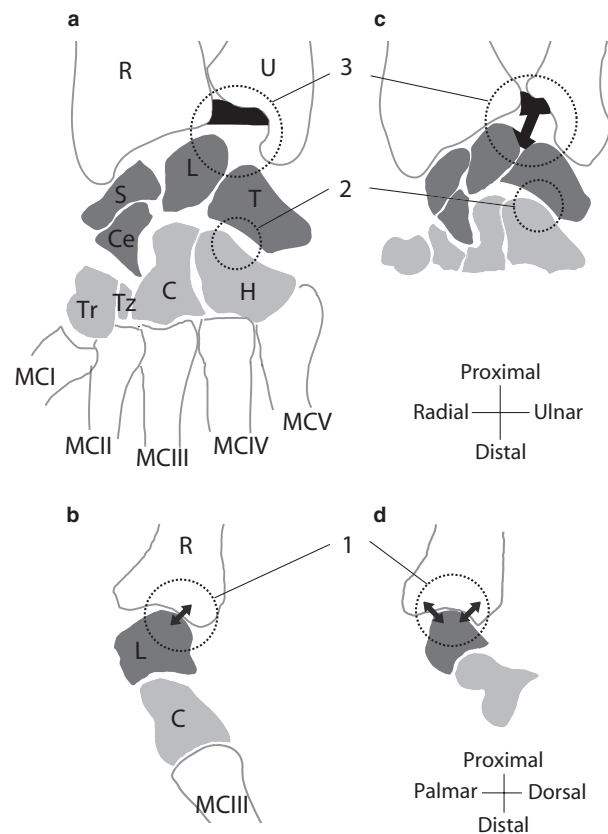


**Fig. 1** Wrist morphology in quadrupedal monkeys; a digitigrade monkey (a, b) and an arboreal quadrupedal monkey (c, d), in both palmar (a, c) and lateral views (b, d). The bones of the proximal carpal row are represented by black silhouettes; the bones of the distal carpal row are represented by grey silhouettes. The main morphological variations between a terrestrial digitigrade monkey and an arboreal quadrupedal monkey concern: (1) congruence of the radius-lunate articulation; (2) morphology of the proximal articular surfaces of the capitate-hamate complex; and (3) the presence/absence of a synovial septum. For details, see the text. Abbreviations: C, capitate; Ce, os centrale; H, hamate; L, lunate; MCI–V, metacarpals I–V; R, radius; S, scaphoid; T, triquetrum; Tr, trapezium; Tz, trapezoid; U, ulna.

1965, 1969, 1971a, 1974, 1985, 1989; Jones, 1967; Ziemer, 1978; Youlatos, 1996; Fig. 1). From a functional point of view, this septum is assumed to limit the radioulnar deviation of the proximal carpal row as well as the deviational movement at the ulnocarpal joint (Cartmill & Milton, 1977; Hamrick, 1996). Consequently, morphological variations of the wrist in ceboid and cercopithecoid quadrupedal monkeys are expected to reflect different patterns of carpal kinematics.

The few studies that have focused on the different roles of the wrist joints in monkeys have provided qualitative descriptions of carpal row mobility (except Jouffroy & Medina, 2002) and osteoarticular columns (for which several carpal bones transmit the joint reaction forces proximodistally as a single functional unit; Schreiber, 1934; Yalden, 1972;

O'Connor, 1975; Ziemer, 1978; Jouffroy & Medina, 2002; Ochsenein, 2002). Studies of carpal row mobility support the hypothesis that mobility occurs primarily at the midcarpal joint during flexion–extension (Schreiber, 1934; Yalden, 1972; Ziemer, 1978) and radioulnar deviation (Schreiber, 1934; O'Connor, 1975; Ziemer, 1978; Jouffroy & Medina, 2002; Ochsenein, 2002). Some of these analyses also support the hypotheses that: first, radial deviation is checked by a radial column (composed of the scaphoid, trapezoid, trapezium, capitate and lunate); second, ulnar deviation is checked by an ulnar column (composed of the capitate, lunate, hamate and triquetrum); and third, flexion–extension is checked by a central column (composed of the lunate and capitate; O'Connor, 1975; Ziemer, 1978). Although these functional studies provide relevant descriptions of carpal bone motion in some monkeys, they do not provide comparative data. In addition, these studies are based on radiographic data in radioulnar and dorsopalmar planes that are not standardised. For instance, the anatomical material used consists of immature specimens (Schreiber, 1934), fresh cadavers, specimens in formalin (O'Connor, 1975; Jouffroy & Medina, 2002; Ochsenein, 2002) or ligamentous preparations (Yalden, 1972; Ziemer, 1978). This lack of standardisation complicates any comparisons because of the possible influence of soft tissues other than ligaments (e.g. tendons or adipose tissue) and behavioural changes that occur during individual development. To avoid these anatomical biases, comparative studies of carpal kinematics in primates should quantify the relative contribution of the midcarpal and antebrachicarpal joints to the overall wrist movement in adult individuals (Jouffroy & Medina, 2002).

The present analysis aims to analyse the extent to which carpal kinematics vary between ceboid and cercopithecoid

quadrupedal monkeys that have varying morphologies. To that end, we first provide new data on carpal kinematics of monkeys (i.e. ceboids and cercopithecoids) that have not been previously investigated. We then describe a new radiographic methodology we have developed that is suitable for the comparative study of the functional morphology of the wrist in primates. This method allows us to describe and compare, quantitatively and qualitatively, the overall mobility of carpal rows as well as the motion of carpal bones during radioulnar deviation and flexion–extension. This study provides new insights on the relationships between the wrist morphology and its functions in primates, especially with regard to locomotor hand postures.

## Materials and methods

Seven wrists of quadrupedal monkeys (ceboids,  $n = 3$ ; cercopithecoids,  $n = 4$ ) were collected from frozen cadavers (Table 1) by removing the forelimb at the glenohumeral joint (*articulatio glenohumeralis*). All specimens were adults with no noticeable pathology and were radiographed with all soft tissues intact. The taxa represented are usually described as quadrupedal. They were divided into three categories according to their preferred substrate (terrestrial, semiterrestrial or arboreal), as well as their preferred locomotor hand postures (Table 1). Although it was not possible to assign a species name to the *Cercopithecus* specimen, it was included in the analysis because the different members of this genus are usually described as palmigrade or palmigrade/digitigrade individuals. Because some specimens were anatomically incomplete, specimen weights were not available. Six specimens were conserved and studied at the Department of Ecology and Biodiversity Management (Département d'écologie et gestion de la biodiversité) in the National Museum of Natural History in Paris, France; the *Papio* specimen was housed and studied at the CNRS primatology station at Rousset-sur-Arc, France.

**Table 1** Comparative sample information: all wrists used in this study were removed from fresh adult cadavers.

	Taxa	Sex	Locomotion and posture		References
			Preferential locomotion substrate	Preferential hand posture	
Olive baboon	<i>Papio anubis</i>	F	Terrestrial	Digitigrady	Rose (1977) Whitehead (1993)
Rhesus macaque	<i>Macaca mulatta</i>	F	Semiterrestrial	Palmigrady/Digitigrady	Rawlins (1993)
Japanese macaque	<i>Macaca fuscata</i>	M	Semiterrestrial	Palmigrady/Digitigrady	Chatani (2003)
Guenon	<i>Cercopithecus</i> sp.	M	Arboreal/Semiterrestrial?	Palmigrady/Digitigrady?	Gautier-Hion et al. (1999)
Bearded saki	<i>Chiropotes satanas</i>	M	Arboreal	Schizodactyl graspwalk	Erickson (1957) Fleagle & Mittermeier (1980) Youlatos (1999)
Grey-necked owl monkey	<i>Aotus trivirgatus</i>	?	Arboreal	Schizodactyl graspwalk	Erickson (1957) Bishop (1964) Youlatos (1999)
Golden-handed tamarin	<i>Saguinus midas</i>	?	Arboreal	Clawed quadrupedalism	Fleagle & Mittermeier (1980) Garber (1991) Hunt et al. (1996)

## X-ray methodology

### Observation planes

Observations were made in two orthogonal planes: the dorsopalmar plane and the radioulnar plane. In order to observe maximum movement at the wrist, each forelimb was disposed with the elbow in a semiflexed posture and the forearm in a semipronated posture (Ziemer, 1978). Four X-ray images were taken of each specimen. Two were taken using a dorsopalmar view, at maximum radial deviation and maximum ulnar deviation. Two were taken using a radioulnar view, at maximum flexion and maximum extension.

### Observation tools

When possible, we used the Faxitron system (Model MX 20 Philips Medical Systems, National Museum of Natural History) because its vertical X-rays provided higher resolution than conventional X-ray methods. This system was very well suited to the observation of small objects such as carpal bones. Image accuracy was also enhanced by using Kodak Industrex X-ray films (ready-pack type, M100 model), which is commonly used in industrial applications. Only the olive baboon specimen (*Papio anubis*) was X-rayed using traditional methods (Model Mobil X ray Generator Saxo) because it was preserved at a different location. The device settings and film development parameters are given in Table 2.

The forelimbs were directly attached to the X-ray films (with the Faxitron system) or plates (with conventional apparatus). The antebrachial and metacarpal bones were immobilised to avoid any influence on the natural motion of the carpal bones. Finally, the X-ray images were digitised at 600 dpi.

### Quantitative analysis: axes and angular measurements

The angles between the two carpal rows and the reference axes were measured at each stationary wrist posture in a dorsopalmar and a radioulnar view. Three reference axes were defined in the dorsopalmar view (for illustrations, see Fig. 2). First, the antebrachial axis (Ab) was perpendicular to the bistyloid axis, linking the radial and ulnar styloid processes. Second, the scaphoid-triquetrum axis (ST) was the axis of the proximal carpal row and was perpendicular to the axis that linked the furthest distoulnar point of the triquetrum to the furthest distoradial point of the scaphoid. The definitions of the 'Ab' and 'ST' axes are given in Jouffroy & Medina (2002). Third, the axis of the dis-

tal carpal row (Cd) was the axis perpendicular to the distal surface of the capitate. Three reference axes were also defined in a radioulnar view: first, the radial axis (R) was perpendicular to the axis of the distal articular surface of the radius; second, the lunate axis (L) was perpendicular to the axis of the distal articular surface of the lunate; and third, the capitate axis (C) was perpendicular to the axis of the distal articular surface of the capitate.

Based on the reference axes, six angles were measured for each specimen with ImageJ software (Abramoff et al. 2004; Fig. 2). In a dorsopalmar view, the angles between Ab and Cd (Ab–Cd), Ab and ST (Ab–ST), and ST and C (ST–Cd) were measured at maximum ulnar deviation (UD) and maximum radial deviation (RD). In a radioulnar view, we measured the angles between R and C (RC), R and L (RL), and L and C (LC) at maximum flexion (F) and maximum extension (E).

Based on the angle measurements, we expressed the movements of the carpal rows as percentages of the overall wrist mobility. During radioulnar deviation, the antebrachiocarpal and midcarpal mobilities, respectively, were expressed as follows:  $(RUD_{Ab-ST}/RUD_{Ab-Cd}) \times 100$  and  $(RUD_{ST-Cd}/RUD_{Ab-Cd}) \times 100$ , with  $RUD$  (total radioulnar deviation) =  $RD$  (total radial deviation) –  $UD$  (total ulnar deviation), in which  $RUD_{Ab-ST}$ : total radioulnar deviation at the antebrachiocarpal joint;  $RUD_{ST-Cd}$ : total radioulnar deviation at the midcarpal joint; and  $RUD_{Ab-Cd}$ : total radioulnar deviation of the wrist. During flexion–extension, the degrees of antebrachiocarpal and midcarpal mobility, respectively, were expressed as  $(FE_{RL}/FE_{RC}) \times 100$  and  $(FE_{LC}/FE_{RC}) \times 100$ , with  $FE$  (total flexion–extension) =  $E$  (total extension) –  $F$  (total flexion), in which  $FE_{RC}$ : total flexion–extension of the wrist;  $FE_{RL}$ : overall flexion–extension at the antebrachiocarpal joint; and  $FE_{LC}$ : total flexion–extension at the midcarpal joint.

The estimation of the accuracy of the quantitative approach was based on the calculation of 95% confidence intervals (CIs). The complete series of angles were measured 10 times for each specimen, each time by the same person. In addition, we determined which angle measurements were the most accurate, choosing between  $RUD_{Ab-ST}$  and  $RUD_{ST-Cd}$ , and between  $FE_{RL}$  and  $FE_{LC}$ . To that end, we tested whether the mean error that resulted from measuring the first angle (i.e.  $RUD_{Ab-ST}$  and  $FE_{RL}$ ) was lower or higher than the mean error that resulted from measuring the second angle (i.e.  $RUD_{ST-Cd}$  and  $FE_{LC}$ ). We calculated the proportion of deviation from the mean for each of the two angles (i.e.  $|x_{ij} - E(x_j)|/|E(x_j)|$ , where  $x_{ij}$  is the  $i$ th measure of the individual  $j$ ). This method scaled the errors within a specimen  $j$  and allowed us to compare the paired series of errors that resulted from measuring each of the angles. These distributions were absolute errors and were therefore not normally distributed. We thus used a non-parametric Wilcoxon

**Table 2** Settings for the radiological protocols. Interspecies variation in bone density required variations in the voltage applied and the duration of exposure to radiation, ranging from 180 s at 35 kV for the grey-necked owl monkey (*Aotus trivirgatus*) to 210 s at 42 kV for the Japanese macaque (*Macaca fuscata*).

X-ray generators	X-ray generator parameters			Radiograph development parameters		
	Amperage (mA)	Voltage (mV)	Exposure (s)	Revelation (s)	Rinsing (s)	Fixation (s)
Faxitron system	10	35.10 <sup>6</sup> –42.10 <sup>6</sup>	180–210	480	120	600
Traditional radiographic system	15	40	Automatic (immediate)	15	180	240



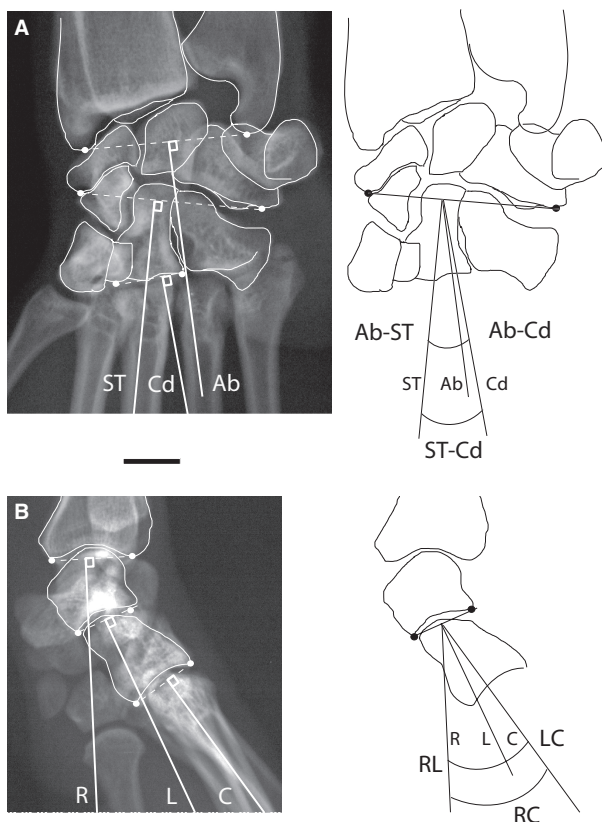


**Fig. 2** Reference axes (right) and angle measurements (left) in: (A) the dorsopalmar view; and (B) the radioulnar view (bottom); the olive baboon (*Papio anubis*) is used as an example. (A) Dorsopalmar view, with Ab, antebrachial axis; Cd, the distal carpal row axis; ST, axis of the proximal carpal row. Ab-Cd, angle between Ab and Cd; Ab-ST, angle between Ab and ST; ST-Cd, angle between ST and C. (B) Radioulnar view, with C, capitate axis; L, lunate axis; R, radial axis. LC, angle between L and C; RC, angle between R and C; RL, angle between R and L. Scale bar: 10 mm. For definitions, see the text.

test to compare the two series of errors (Wilcoxon test in R version 2.10.1).

### Qualitative analysis

We visually evaluated carpal bone motion and areas of maximum bone contact by assessing spacings at the antebrachiocarpal joints and proximal intercarpal joints. For radioulnar deviation, we described variations in spacing between the radius and lunate, between the radius and triquetrum, and between the ulna and triquetrum. In addition, we compared the scaphoid-lunate spacing with the lunate-triquetrum spacing. For flexion-extension, we described bone congruences in the central osteoarticular column (radius-lunate joint and lunate-capitate joint).

To that end, contours of the carpal and antebrachial bones were made from each radiograph and then superimposed using the antebrachial bone contours as a reference. The motion of the carpal bones achieved between each posture of maximum movement (radial deviation, ulnar deviation, flexion and extension, proximal and distal shifts) was described. The joint

postures for which articulating carpal bones shared a maximum area of contact were also recorded. These postures provided the greatest joint stability (i.e. close-packed position) and were assumed to optimise the weight-bearing functions of the wrist. The close-packed position suggests that any movement away from this position reduces contact areas and joint stability, leading to a loose-packed position.

### Results

The results regarding the mobility of the carpal rows during radial and ulnar deviation and during flexion and extension are given in absolute (degree) and relative values (percentage) in Table 3. These results are respectively summarised in Fig. 3a–d. Qualitative results for the two movements are given in Table 4 (carpal bone motion) and Table 5 (areas of maximum bone contact and joint spacings). The qualitative results for radioulnar deviation are illustrated in Fig. 4, while Fig. 5 provides a summary of our observations. Significant examples of flexion-extension are shown in Fig. 6.

### Accuracy estimation of the quantitative approach

For each of the repeated measurements, 95% CIs for normally distributed variables are calculated. Overall, the error in measurements is uniformly distributed among taxa and does not depend on specimen size (Table 3; Fig. 3). Errors in measurement are not affected by the observation planes; however, errors seem proportionally larger when smaller angles are measured. We therefore determined which angle measurements are the most accurate, choosing between  $RUD_{Ab-ST}$  and  $RUD_{ST-Cd}$ , and between  $FE_{RL}$  and  $FE_{LC}$ . These angles estimate the overall mobility of the two carpal rows during radioulnar deviation and flexion-extension. To that end, a comparison of the mean errors associated with angle measurements shows that the measurement of  $RUD_{ST-Cd}$  is more accurate than the measurement of  $RUD_{Ab-ST}$  ( $P = 0.00014$ ), and that the measurement of  $FE_{LC}$  is more accurate than the measurement of  $FE_{RL}$  ( $P = 6.9 \times 10^{-5}$ ). Because the angle measurements for the distal carpal row are the most robust (Table 3), we choose to present only the contribution of  $RUD_{ST-Cd}$  and  $FE_{LC}$  to the overall wrist movements, as seen in Fig. 3c,d.

### Radioulnar deviation

Quantitative results (both relative and absolute) show that neither the cercopithecoids nor the ceboids are characterised by clear functional tendencies (Fig. 3a,c).

For all taxa studied, a large part of the radioulnar movement occurs at the midcarpal joint. This distribution is indicated by  $RUD_{ST-Cd}/RUD_{Ab-Cd} 100$ , which is  $> 50\%$  (Table 3; Fig. 3a,c). This ratio is substantially variable, ranging from about 60% to 80%. In ceboids, the lowest degree of midcarpal mobility is found in *Saguinus midas* (60.1%), while the highest is found in *Aotus trivirgatus* (78.2%). The value for

**Table 3** Angle measurements for Ab-Cd, Ab-ST, ST-Cd, RC, RL and LC (in degrees) are given for radial deviation (RD), ulnar deviation (UD) extension (E) and flexion (F). Angle values are negative when they are clockwise and positive when they are counterclockwise. These raw data were used to calculate the total amplitudes of radioulnar deviation (RUD) and flexion-extension (FE). Based on these values, we calculated the midcarpal contribution to overall radioulnar deviation,  $(RUD_{ST-Cd}/RUD_{Ab-Cd}) \times 100$ , and the midcarpal contribution to overall flexion-extension,  $(FE_{LC}/FE_{RC}) \times 100$ . The most robust measurements are in bold. Including angle values (ST-Cd, LC) and the relative contributions of the distal carpal rows to total wrist mobility (RUDST-Cd/RUDAb-Cd)  $\times 100$ . Confidence intervals at 95% are in parentheses. For abbreviations and definitions, see the text.

RD	UD				RUD				E				F				FE				FE <sub>LC</sub> /FE <sub>RC</sub> (%)
	Ab-Cd	Ab-ST	ST-Cd	Ab-Cd	Ab-ST	ST-Cd	Ab-Cd	Ab-ST	ST-Cd	RUD <sub>ST-Cd</sub> /RUD <sub>Ab-Cd</sub> (%)	RC	RL	LC	RC	RL	LC	RC	RL	LC		
<i>Saguinus midas</i>																					
Mean	-19.3	-11.5	-7.9	39.2	11.9	27.5	58.5	23.4	35.4	60.1	61.7	46.2	15.3	-38.4	7.7	-46	100.1	38.5	61.3	61.2	
Max	-25	-13	-13	42	13	31	65	26	44	74	67	49	19	-46	14	-54	108	45	70	67	
Min	-16	-7	-4	36	8	23	54	15	28	51	59	43	11	-29	3	-37	89	32	60	54	
CI	1.5	1.1	1.9	1.2	0.9	1.6	1.9	1.9	2.9	3.7	1.4	1.5	1.7	3.2	2.0	3.2	3.7	2.9	4.4	3.2	
<i>Aotus trivirgatus</i>																					
Mean	-7.0	-8.9	2.2	19.8	-3.6	22.9	26.8	5.3	20.9	78.2	69.6	47.8	21.5	-59	6.5	-65.2	128.6	41.3	86.7	67.4	
Max	-9	-13	4	24	-5	26	29	9	23	92	76	53	26	-63	9	-69	134	44	91	69.8	
Min	-5	-5	0	17	-2	21	25	2	18	69	63	44	17	-54	5	-60	121	38	79	64.4	
CI	0.9	1.5	0.8	1.4	0.8	0.9	1.1	1.5	1	4.7	3	1.7	2	1.7	0.9	1.7	2.6	1.1	2.2	1	
<i>Chiropterus satanas</i>																					
Mean	-18.2	-12.5	-5.5	42.1	6.4	35.8	60.3	18.9	41.3	68.4	78.1	24.9	52.7	-91.2	-36.2	-54.5	169.3	61.1	107.2	63.4	
Max	-23	-17	-9	48	8	40	66	24	48	73.8	85	30	57	-94	-48	-60	176	70	113	68.9	
Min	-15	-8	-3	35	5	29	52	16	34	62.5	72	21	49	-85	-25	-45	164	51	98	58.3	
CI	1.7	1.5	1.5	2.5	0.7	2	3	1.7	2.7	2.2	2.1	1.7	1.5	1.9	3.8	3.1	2.5	3.3	2.8	1.9	
<i>Cercopithecus</i> sp.																					
Mean	-12	-19.5	7.6	40.5	1.6	39.4	52.5	20.7	31.8	60.6	53.2	33.5	19.4	-74.5	-24.7	-49.9	127.7	58.2	69.3	54.3	
Max	-13	-21	10	45	4	41	58	24	34	68	60	39	25	-78	-27	-53	134	65	75	59.1	
Min	-10	-18	5	37	0	36	50	16	28	54.9	49	27	16	-70	-18	-47	120	51	64	50	
CI	0.7	0.8	1	1.4	0.8	1	1.7	1.6	1.2	2.2	2	2.5	1.9	1.4	1.7	1.4	2.2	2.8	2.2	1.8	
<i>Macaca fuscata</i>																					
Mean	-20.7	-17.1	-3.8	17.8	-4.6	21.5	38.5	12.5	25.3	65.8	71.3	49.2	22	-68.7	-3.3	-67.8	140	49.7	89.8	64.1	
Max	-24	-18	-7	22	-6	23	45	15	29	72.5	77	51	27	-76	-6	-72	147	56	95	67.9	
Min	-18	-16	-1	15	-3	20	34	11	22	60	66	47	16	-63	-1	-61	133	44	83	61.9	
CI	1.2	0.4	1.4	1.2	0.5	0.5	2.1	0.8	1.5	2.5	2.3	0.7	2.4	2.3	1.4	2.1	2.2	2.5	2.7	1.4	
<i>Macaca mulatta</i>																					
Mean	11	-8	19	26.0	-5.2	31.3	15	3	12.3	81.3	59.2	35.7	23.6	-55.9	-7.6	-48.8	115.1	42.9	72.4	62.9	
Max	14	-11	22	29	-7	34	19	5	14	93	61	39	27	-61	-14	-61	119	48	83	70.9	
Min	7	-5	16	23	-4	29	12	1	10	68.8	58	33	19	-51	-20	-42	112	35	67	58.3	
CI	1.2	1.1	1.2	1.0	0.6	1.1	1.4	1	1	4.8	0.9	1.1	1.4	1.8	2.6	3.5	1.4	2.5	3	2.4	
<i>Papio anubis</i>																					
Mean	-16.3	-23.5	7	44.0	2.8	41.1	60.3	24.9	35.3	58.4	31.2	26.3	5.2	-74	8.9	-83.1	105.2	17.4	87.7	83.4	
Max	-21	-25	11	47	4	43	64	27	44	68.8	38	31	8	-77	12	-87	110	21	92	89.2	
Min	-12	-22	3	41	2	37	57	20	30	52.6	26	19	1	-67	3	-76	101	11	79	78.2	
CI	1.9	0.6	1.9	1	0.6	1.1	1.7	1.5	2.7	3	2	2.4	1.7	2.1	1.7	2.2	1.8	2	2.7	2.2	

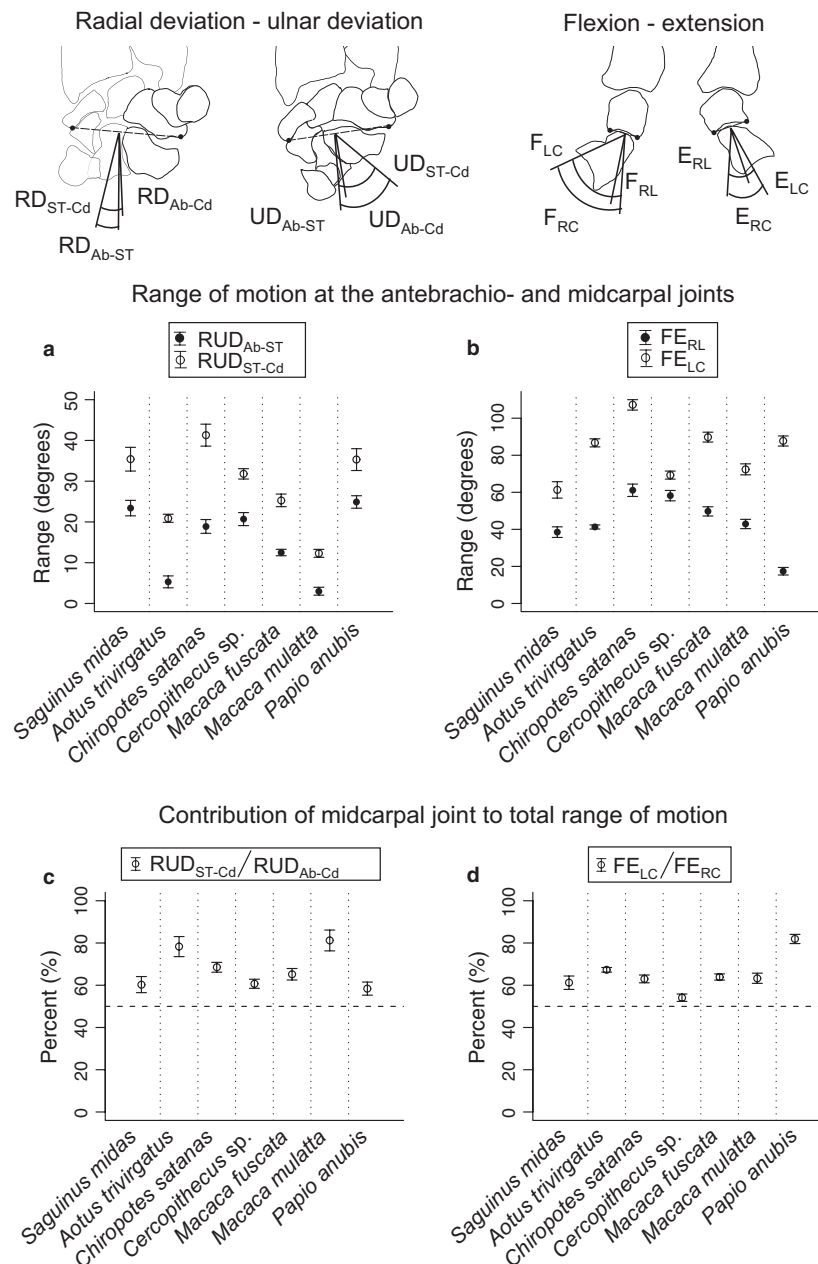


**Fig. 3** Overall range of motion at the wrist joints in radioulnar deviation (a) and flexion–extension (b), and percent contribution of midcarpal mobility to (c) total radioulnar deviation ( $\text{RUD}_{\text{ST-Cd}}/\text{RUD}_{\text{Ab-Cd}}$ ) 100 and (d) total flexion–extension ( $\text{FE}_{\text{LC}}/\text{FE}_{\text{RC}}$ )  $\times$  100. Error bars represent the 95% CIs. For abbreviations, see the text.

*Chiropotes satanas* is intermediate (68.4%). Cercopithecoids display almost the same degrees of variation in the percent contribution of the midcarpal joint, with the lowest value found for *Papio anubis* (58.4%) and the highest value found for *Macaca mulatta* (81.3%). The values for *M. fuscata* (65.8%) and *Cercopithecus sp.* (60.6%) are intermediate.

A comparison between the relative and absolute mobilities of the carpal rows allows identification of two main results in terms of variation: first, *Aotus trivirgatus* and *Macaca mulatta* share the highest percentages of midcarpal

contribution (with similar values) and the lowest overall mobility of the carpal rows. Second, the rhesus macaque differs from the Japanese macaque in the midcarpal contribution to overall wrist deviation, which is approximately 16% higher in the rhesus macaque (81.3% in *M. mulatta*, 65.8% in *M. fuscata*), and in overall midcarpal mobility, which is 50% lower in the rhesus macaque (12° in *M. mulatta*, 25° in *M. fuscata*).

With regard to our qualitative results, the cercopithecoids and the ceboids have a similar pattern of carpal bone

**Table 4** Substantial carpal bone motion observed during radioulnar deviation and flexion–extension.

RD → UD				F → E	
Proximal carpal bones		Distal carpal bones		Lunate	Capitate
<i>Saguinus midas</i>				E + pS	E + pS
S, Ce, L	UD + dS	Tp, Tz, C	UD + dS		
T, P	UD + pS	H	UD + pS		
<i>Aotus trivirgatus</i>					
S, Ce, L	UD + dS	Tp, Tz, C	UD + dS		
T, P	UD + pS	H	UD + pS		
<i>Chiropotes satanas</i>					
S, Ce, L	UD + dS	Tp, Tz, C	UD + dS		
T	UD + pS?	H	UD + pS		
P	UD + pS				
<i>Cercopithecus</i> sp.					
S, Ce, L	UD + dS	Tp, Tz, C	UD + dS		
T, P	UD + pS	H	UD + pS		
<i>Macaca fuscata</i>					
S, Ce, L	dS	Tp, Tz, C	UD + dS		
T	UD + pS	H	UD + pS		
P	pS				
<i>Macaca mulatta</i>					
S, Ce	No motion	Tp, Tz, C	UD + dS		
L	UD? + dS ?				
T, P	UD + pS ?	H	UD + pS		
<i>Papio anubis</i>					
S, Ce	dS	Tp, Tz, C	UD + dS		
L	UD + dS				
T, P	UD + pS	H	UD + pS		

C, capitate; Ce, os centrale; dS, distal shift; E, extension; F, flexion; H, hamate; L, lunate; P, pisiform bone; pS, proximal shift; RD, radial deviation; S, scaphoid; T, triquetrum; UD, ulnar deviation.

motion. Indeed, radial deviation involves a proximal shift of the scaphoid/os centrale, lunate, trapezium/trapezoid and capitates in all specimens (Table 4, Fig. 4). At the end of the radial deviation, the scaphoid/os centrale, trapezium/trapezoid, lunate and capitate adopt maximum congruence. During ulnar deviation, only the bones of the ulnar column are proximally shifted, such that the ulna, triquetrum, pisiform and hamate are engaged in maximum congruence at the end of the movement. Despite this common pattern, the macaques and the baboon exhibit less mobility (UD) at the proximal part of their radial osteoarticular column than do the other taxa.

With regard to the interarticular spaces, the ceboids differ from the cercopithecoids in two characteristics (Table 5; Fig. 4). During radial deviation, the lunate in ceboids comes exclusively into contact with the radius and has no contact with the triangular ligament. In this posture, ceboids are also characterised by a scaphoid-lunate space that is either similar to the lunate-triquetrum spaces (*Saguinus midas* and *Aotus trivirgatus*) or narrower than the lunate-triquetrum spaces (*Chiropotes satanas*). The ulna-triquetrum interarticular space appears almost unchanged with radial deviation. In ulnar deviation, the triquetrum comes into contact with the radius in *Saguinus midas* and *Chiropotes satanas*. In cercopithecoids, radial deviation involves the lunate coming into contact with the triangular ligament, and the lunate/scaphoid spacing is wider than the lunate/triquetrum spacing. Cercopithecoids, however, show two variations. During ulnar deviation, the triquetrum does not touch the radius, as in *Aotus trivirgatus*. Additionally, with the exception of *Macaca mulatta*, the cercopithecoids display an enlargement of the ulna-triquetrum spaces during radial deviation.

To summarise, in Fig. 5, we list the main qualitative kinematic variations that describe the differences between ceboids and cercopithecoids. The ceboids are characterised by:

**Table 5** Major differences in interarticular joint spaces.

Taxa	Radioulnar deviation				Flexion–extension	
	Radial deviation		Ulnar deviation		Flexion	Extension
	Proximal L contact (Fig. 4 – feature 1)	Comparisons between LT and SL (Fig. 4 – feature 2)	TR contact (Fig. 4 – feature 3)	UT contact (Fig. 4 – feature 4)	Comparisons between RL and LC (Fig. 6)	
					RL	LC
<i>Papio anubis</i>	Radius + triangular ligament	LT < SL	Absence	Reduction	RL: large	RL: narrow
<i>Macaca mulatta</i>	Radius + triangular ligament	LT < SL	Absence	Subequal	LC: narrow	LC: narrow
<i>Macaca fuscata</i>	Radius + triangular ligament	LT < SL	Absence	Reduction	palmarly	dorsally
<i>Cercopithecus</i> sp.	Radius + triangular ligament	LT < SL	Absence	Reduction		
<i>Chiropotes satanas</i>	Radius exclusively	LT > SL	Presence	Subequal		
<i>Aotus trivirgatus</i>	Radius exclusively	LT = SL	Absence	Subequal		
<i>Saguinus midas</i>	Radius exclusively	LT = SL	Presence	Subequal		

L, lunate; LC, lunate-capitate spacing; LT, lunate-triquetrum spacing; RL, radius-lunate spacing; SL, scaphoid-lunate spacing; TR, triquetrum-radius contact; UT, ulna-triquetrum contact.



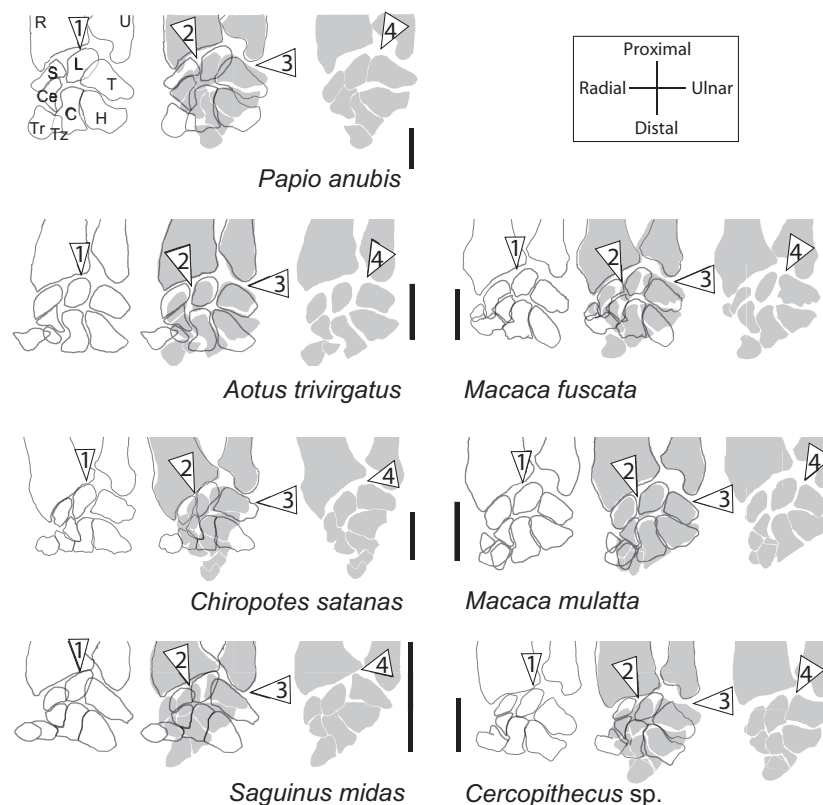


**Fig. 4** Carpal bone motion during radioulnar deviation in the seven wrists of non-hominoid anthropoids; the superimpositions of carpal bone contours are drawn from dorsopalmar radiographs during radial deviation (white contours) and ulnar deviation (black silhouettes). Four characteristics distinguish ceboids from cercopithecoids: (1) radius-lunate spacing; (2) scaphoid-lunate spacing relative to lunate-triquetrum spacing; (3) ulna-triquetrum spacing; and (4) radius-triquetrum spacing. To simplify the diagram, the contours of the pisiform bone were deleted. Abbreviations are as in Fig. 1. Scale bar: 10 mm.

limited movement of the carpus at the ulna-triquetrum joint; increased mobility of the scaphoid/os centrale complex; and absence of direct contact between the triangular ligament and the lunate bone. Additionally, ulnar deviation generates radius-triquetrum contact in *Chiropotes satanas* and *Saguinus midas*. The cercopithecoids display: substantial movement of the carpus at the ulna-triquetrum joint; limited deviational movements of the scaphoid/os centrale complex; and direct contact between the triangular ligament and the lunate bone during radial deviation. Finally, although the *Cercopithecus* sp. specimen mainly shows cercopithecoid-like carpal kinematics (areas of maximum bone contact), it also shows greater mobility of the proximal radial osteoarticular column, as we observed in the ceboids.

### Flexion–extension



Quantitative results (both relative and absolute) show that neither cercopithecoids nor ceboids are characterised by clear functional tendencies (Table 3; Fig. 3b,d).

Our results for all the taxa studied show that a large part of the mobility during flexion–extension occurs at the midcarpal joint (Table 3; Fig. 3d). For this ratio, ceboids do not

differ from cercopithecoid taxa. The variation in midcarpal mobility in cercopithecoids – ranging from 54.1% in *Cercopithecus* sp. to 81.9% in *Papio anubis*, including 63.9% in *M. fuscata* and 63.3% in *M. mulatta* – is more than four times greater than the variation in ceboids – ranging from 61.2% in *Saguinus midas* to 67.3% in *Aotus trivirgatus*, including *Chiropotes satanas* (at 63%).

A comparison between the relative and absolute mobilities of the carpal rows allows the identification of two characteristics that distinguish *Papio anubis* from the other monkeys. Indeed, the *Papio anubis* specimen exhibits a substantially larger contribution by the midcarpal joint to overall wrist mobility than the other anthropoids (Table 3; Fig. 3d). Additionally, the *Papio anubis* specimen has the lowest absolute antebrachioarticular mobility (approximately 17°) among the monkeys studied (ranging from 38° to 51°), while its midcarpal mobility (88°) falls within the overall variation of other taxa (ranging from 61° to 107°). This particularity is likely related to the low degree of overall mobility in extension found in *Papio anubis* (31°) as compared with the other monkeys (53°–78°).

Our qualitative analysis focused on carpal bone motion and joint congruences of the central osteoarticular column.

	Ceboids		Cercopithecoids	
Columns	Radial	Ulnar	Radial	Ulnar
Bone motions	Proximal shift and deviation: scaphoid/os centrale lunate trapezoid/trapezium capitate		Proximal shift of carpal bones: as in ceboids Deviation: scaphoid and os centrale with low mobility except in <i>Cercopithecus</i> sp.	
Intercarpal joint spacings	Lunate exclusively in contact with the radius		Lunate in contact with the triangular ligament and the radius	Lunate exclusively in contact with the radius
	2/3 specimens show a radius-triquetrum contact			
	Ulna-triquetrum space does not vary substantially		Ulna-triquetrum space vary except in <i>M mulatta</i>	
Examples	Lunate-triquetrum space $\geq$ Lunate-scapoid space		Lunate-triquetrum space $<$ Lunate-scapoid space	
	 <i>Chiropotes satanas</i>		 <i>Papio anubis</i>	

**Fig. 5** Characteristics of the radial and ulnar osteoarticular columns in the wrist in ceboids and cercopithecoids. Black silhouettes represent the carpal bones that contribute most to wrist stability; white contours represent the carpal bones that contribute least to wrist stability. NB: in cercopithecoids, the lunate-capitate complex contributes to wrist stability during both radial and ulnar deviation.

These results show that all specimens share a common functional pattern, independent of their taxonomy or their locomotor hand postures. At the antebrachio-carpal joint, extension is associated with an extension and proximal shift of both the lunate and capitate (Table 4; Fig. 6). In terms of joints spacings, maximum extension leads to the maximum congruence of the proximal articular surface of the lunate with the dorsal portion of the distal articular radial surface (Table 5). During flexion, this joint is 'loosely packed' (*sensu*; Ziemer, 1978). At the midcarpal joint level, a narrow interarticular space is maintained between the proximal articular surfaces of the capitate and the lunate during both flexion and extension.

## Discussion

We present a new methodology suitable for the comparative analysis of primate carpal kinematics that takes into account the 'row' and 'column' concepts. Using this new method, we provide new quantitative and qualitative data on carpal kinematics in seven species of quadrupedal monkeys. Our results help to characterise different patterns of carpal kinematics among quadrupedal monkeys and contribute to a better understanding of the relationships between the mobility of the wrist, its morphology and its role in locomotor hand postures.

## Reliability and limits of the methodology

Because of the lack of standardised and comparative data on carpal kinematics in primates, we develop a new methodology suitable for this study. Therefore, a discussion of the comparability of data is required to allow us to assess the significance of these data for our understanding of the relationships between the function and morphology of the wrist in monkeys. In the present study, the comparability of the data depends on the relevance of the method used; its accuracy; the role of individual variation; and the impact of studying fresh cadavers instead of live individuals.

First, we analyse carpal bone motion in two well-identified reference planes, although these bones also achieve conjoint out-of-plane motion, in practice (i.e. rotation, radio-ulnar deviation and flexion-extension; Moojen et al. 2002; Orr et al. 2010). In this study, this kind of motion is signalled in all specimens by variation in the shape of carpal bone contours between two maximum wrist postures (Figs 4 and 6). For example, ulnar deviation in *Cercopithecus* sp. involves a mediolateral reduction of the lunate silhouette (Fig. 4), while extension involves an increase in its height (Fig. 6); however, out-of-plane motion of the central column in cadavers and living individuals remains relatively limited during flexion-extension. For instance, in the wrist of a living human, a 120° flexion-extension angle of the capitate is associated with 0.8° of pronosupination and

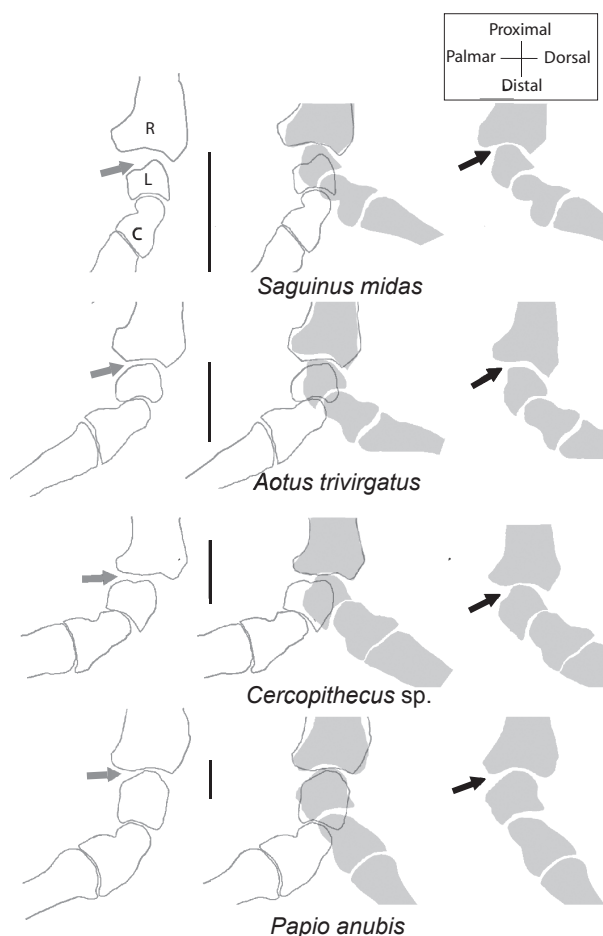


**Fig. 6** Radiographs in a radioulnar view of carpal motion of the osteoarticular column of flexion–extension in four anthropoids; the superimpositions of carpal bone contours are drawn from radioulnar radiographs during flexion (white contours) and extension (black silhouettes). Note the proximal shift of the lunate-capitate complex during extension. Arrows indicate the degree of articular congruence between the proximal articular surfaces of the lunate and the distal articular radial surface. Black arrows indicate a narrow radius-lunate interarticular space; grey arrows indicate a wide radius-lunate interarticular space. Abbreviations are as in Fig. 1. Scale bar: 10 mm.

16.2° of radioulnar deviation, while a 58° angle of flexion–extension of the lunate is associated with 2.5° of pronosupination and 12° of radioulnar deviation (Moojen et al. 2002). In non-human primates, this small amount of out-of-plane motion at the central column is sometimes accompanied by substantial mobility at the proximal intercarpal joints (e.g. *Pan*), which contributes to central column stability (Orr et al. 2010). With regard to radioulnar deviation, out-of plane movements are substantial, especially at the proximal intercarpal joints. For instance, during a 20° radial deviation, the proximal bones (scaphoid and lunate and triquetrum) achieve an approximately 8°–15° of flexion, while they achieve 20°–24° of extension during a 20° ulnar deviation (Moojen et al. 2002). Because all proximal carpal

bones experience similar out-of-plane motion (flexion in radial deviation and extension in ulnar deviation) at similar magnitudes, we estimate that out-of-plane movements of carpal bones measured between maximum radial deviation and maximum ulnar deviation compensate and thus do not substantially affect the ‘in-plane’ carpal movements studied here.

Second, we show that neither the specimen size nor the observation planes seems to affect the error in measurements. This approach is thus compatible with comparative studies; however, error in measurements seems proportionally larger when smaller angles are measured. For instance, the angle measurements for the distal carpal row are significantly more robust than those for the proximal row. Therefore, the results of this study suggest that any quantitative comparison of carpal kinematics in primates should primarily focus on the most mobile joints in order to limit the error in measurements.

Third, in this comparative perspective, given the small number of specimens representing each taxon in the present study, interindividual variation could explain differences between individuals of different taxa. As an example, the midcarpal contribution to overall radioulnar deviation in the two *Macaca* specimens studied here differs by approximately 16% (81.3% in *M. mulatta*; 65.8% in *M. fuscata*; Table 3; Fig. 3c). These results suggest that contributions of wrist joints to the total range of motion show a high degree of variation at an intragenetic level (here, in *Macaca*). Such a variation is also observed in hominoids, as can be seen when one calculates midcarpal contribution to overall radioulnar deviation (as a percentage) based on available data from previous studies (Sarmiento, 1988; Jouffroy & Medina, 2002; e.g. 20% in *Hylobates* and *Homo*). Nevertheless, at a suprafamilial level (ceboid, cercopithecoid and hominoid), although a high degree of variation is observed (whatever the source, which can include sex, behaviour or taxonomy), functional tendencies can be characterised.

Fourth, the use of passive and unloaded wrist specimens collected from cadavers could limit the relevance of this study for understanding wrist functions in living primates; however, comparative analyses of wrist motion do not show a significant difference between *in vivo* weight-bearing conditions and passive and unloaded conditions. Indeed, cineradiographic and radiographic images of the wrist in quadrupedal and suspended anthropoids have highlighted a similarity in carpal rotation under loaded and unloaded conditions (Jenkins & Fleagle, 1975; Jenkins, 1981). Similarly, in humans, it has been shown that carpal kinematics described from static analyses remains very close to those described from dynamic analyses (Kobayashi et al. 1997; Neu et al. 2001; Moojen et al. 2002; Moore et al. 2007). Therefore, passive and unloaded wrist specimens can be used to investigate *in vivo* functions of the primate wrist.

### Relationships between carpal kinematics and wrist morphology in quadrupedal monkeys

This study is designed to assess the extent to which carpal kinematics vary between ceboid and cercopithecoid quadrupedal monkeys with varying morphologies. A comparison of the absolute and relative mobility of the two carpal rows shows few clear variations between ceboids and cercopithecoids in radioulnar deviation and flexion–extension. The midcarpal contribution to overall wrist mobility is predominant compared with the antebrachiocarpal contribution in all quadrupedal monkeys. In addition, our results do not support the hypothesis that baboons benefit from a better congruence of the radius–lunate joint in extension or that cercopithecoids have a limited radioulnar deviation at the midcarpal joint. In contrast, our analysis highlighted two kinematic variations in ceboids and *Papio anubis* that illustrate a relationship between carpal kinematics and morphology.

First, ceboids of the present study are characterised by an ulnar column that is proximally not very mobile and that is better stabilised than the proximal radial column, while the reverse is observed in the cercopithecoids; this pattern strongly suggests that the synovial septum has direct implications for carpal kinematics in arboreal quadrupedal monkeys.

Second, our quantitative results for flexion–extension show that *Papio anubis* differs from the other taxa in its limited mobility at the antebrachiocarpal joint. This particularity is likely related to the low degree of overall mobility in extension found in *Papio anubis* as compared with the other monkeys. This result suggests that exclusively digitigrade species are characterised by an extension limitation system that is most likely a result of the radial dorsal process that projects into the depression of the scaphoid and the presence of an intraarticular meniscus between the dorsal parts of the radius and scaphoid.

These two patterns of carpal kinematics must, however, be regarded only as tendencies for two reasons. For example, although the wrists of *Macaca mulatta* and *Cercopithecus* (characterised by the absence of a synovial septum) mainly exhibit cercopithecoid-like carpal kinematics in radioulnar deviation, they also display some ceboid-like characteristics (i.e. invariant ulnocarpal contact and substantial mobility of the proximal radial osteoarticular column). Similarly, we highlighted that *Aotus trivirgatus* and *Macaca mulatta* differ from other taxa in having the highest midcarpal contribution to overall wrist mobility and the lowest overall mobility of the wrist. Nevertheless, these results confirm that differences in carpal kinematics among quadrupedal monkeys are not systematically related to taxonomy. Such differences could also be related to functional adaptations of the hand at the species level. To this end, new comparative studies of monkey wrists are required in order to test whether these variations in carpal kinematics are related to morphological variation.

### Relationships between carpal kinematics and hand postures in quadrupedal monkeys

Because locomotor hand postures are defined by the positioning of the forearm's long axis, the interpretation of carpal kinematics in terms of locomotion needs to integrate comparative data on wrist mobility that are calibrated by the forearm's long axis (e.g. Orr et al. 2010); however, such an approach is not possible in this study because of the reduced size of the Faxitron system (for macaque specimens, for example). Regardless, even if this bias limits our functional inferences, our standardised data for carpal kinematics, both relative and absolute, allow us to predict how and where motion occurs at the wrist under weight-bearing conditions.

Our study shows that ulnar deviation in ceboids, which use exclusively arboreal hand postures (i.e. schizodactyl graspwalk, clawed quadrupedalism), is characterised by a proximal ulnar column (ulna–triquetrum joint) that is less mobile than the proximal radial column (radius–scaphoid/os centrale joints), an absence of contact between the triangular ligament and the lunate and, particularly in *Chiropotes* and *Saguinus*, a radius–triquetrum contact. Previous studies have shown that arboreal quadrupedal ceboids achieve high degrees of ulnar deviation of the hand on both terrestrial and arboreal substrates (Lemelin & Schmitt, 1998). During the stance phase, the ulnar column and the pisiform bone form a longitudinal arch, which primarily ensures weight transmission towards and away from the substrate (Grand, 1968). The mobile architecture of the wrist in arboreal quadrupedal monkeys can be adjusted to changes in branch diameter (Ziemer, 1978). Therefore, an ulna–triquetrum joint, the stability of which is improved by the absence of contact between the lunate and the triangular ligament, would help to stabilise the wrist under weight-bearing conditions during ulnar deviation. In this situation, the radius–triquetrum contact that we observed in *Chiropotes* and *Saguinus* would provide a more specialised form of weight transmission that is mainly performed by the ulnar osteoarticular column. Finally, the high degree of mobility of the scaphoid/os centrale complex in relation to the lunate would enable adaptation of the wrist architecture in accordance with the branch diameter.

Our study also provides evidence that the wrists of cercopithecoids, which are involved in digitigrady, either occasionally (*Macaca* sp.) or frequently (*Papio anubis*) have a proximal radial column (radius–scaphoid/os centrale joints) that is less mobile than the ulnocarpal joint, and a lunate that can make contact with both the radius and the triangular ligament. Compared with arboreal quadrupedal monkeys, forelimb morphology in digitigrade species is thought to be better adapted in resisting higher vertical peak forces and medially (vs. laterally) directed forces that result from substrate reaction (Schmitt, 1994; Schmitt & Hanna, 2004). In addition, both occasionally and frequently

digitigrade monkeys achieve much less ulnar deviation of the hands than do strictly palmigrade ceboids (Lemelin & Schmitt, 1998). Therefore, under such conditions, our results support the hypothesis that lower mobility of the radial part of the wrist and a more efficient transmission of weight between the lunate and antebrachial bones (via the triangular ligament) contribute to stabilising the wrist in both occasionally and frequently digitigrade monkeys.

Our results also suggest that exclusively digitigrade monkeys (*Papio anubis*) differ from the other taxa in a limited mobility of the antebrachiocarpal joint in flexion–extension, which is likely a result of the reduction of the overall mobility of the wrist in extension. Previous studies of the overall mobility of the hand have shown that digitigrady involves a reduction of wrist mobility in extension (Jones, 1967; Tuttle, 1969; Richmond, 2006). These results are not strictly comparable with ours because they do not rely on standardised axes of reference; however, previous analyses of overall wrist mobility, as well as the present study, suggest that a high degree of digitigrady might involve a reduction in the antebrachiocarpal contribution to overall extension. Recent biomechanical analyses have highlighted the fact that digitigrady involves an increase in the effective limb length and in step lengths, providing mechanical advantages and a lower cost of transport when walking on terrestrial substrates (Patel, 2009, 2010; Patel & Wunderlich, 2010). Therefore, reduced mobility in the antebrachiocarpal joint in extension might contribute to stabilising the wrist, enabling the monkey to hold the palm of the hand off the substrate during walking; such an adaptation might reduce the energetic cost of the digitigrade walk.

## Conclusions

The purpose of this study is to provide new data on the carpal kinematics of quadrupedal monkeys in order to develop a suitable comparative methodology of the functional morphology of the wrist, and deepen our understanding of the complex relationships between wrist morphology and wrist function in these primates.

We highlight two main results in this respect. First, our quantitative results show that morphological variations that have previously been recognised in quadrupedal monkeys partially affect the relative mobility of their carpal rows. Indeed, all of the monkeys studied display a common pattern of carpal row mobility during radioulnar deviation and flexion–extension, which is characterised by greater mobility of the midcarpal joint than the antebrachiocarpal joint. The olive baboon, however, is characterised by having the lowest antebrachiocarpal mobility for extension. This characteristic is likely the result of a distal radial process and a dorsal intraarticular meniscus that may both limit extension of the proximal carpal row; this functional pattern may be typical of habitual digitigrade species. Second, two functional tendencies are qualitatively identified, confirming that carpal

kinematics may be affected by morphological variations. The synovial septum typical of ceboids involves less mobility and more stability of the ulnar part of the wrist than is seen in cercopithecoid wrists; such a functional variation may reflect locomotor differences between arboreal quadrupedal taxa (ceboids) and digitigrade taxa (cercopithecoids).

From a methodological point of view, the ‘row’ and ‘column’ concepts have thus helped to improve our knowledge of the functional morphology of the anthropoid wrist, despite its considerable complexity and variability. The various patterns of carpal kinematics found in quadrupedal monkeys are differentiated based on the relative and absolute contributions of the carpal joints. Such knowledge should be extended to as-yet unresearched taxa. Generally speaking, the present study supports the hypothesis that the functional morphology of articular systems can be understood if one takes into account the absolute and relative mobility of all of its joints. As a consequence, we propose that the approach presented in this paper be extended to other articular systems.

## Acknowledgements

We gratefully acknowledge all of our colleagues, who contributed to this research effort in various ways. We are indebted to Drs Françoise K. Jouffroy, K. d’Août, A. Balzeau and S. Pavard for sharing comments and suggestions throughout the course of this research project. We also wish to thank anonymous reviewers and the receiving editor for their advice. Many thanks to Ilona Bossanyi and Dr Sally Reynolds, as well as the editing reviewer and a reviewer from Elsevier webshop, for their help with the English editing. Access to collections (except for *Papio anubis*) and to the Faxitron systems was provided courtesy of Eric Pellé from UMR 7179 (MNHN/CNRS) and P. Pruvost from the Department of Collections at the National Museum of Natural History. The *Papio anubis* specimen was obtained and radiographed (Mobil X ray Generator SAXO) with the permission of Guy Dubreuil, Head of the CNRS Primatology station at Rousset-sur-Arc. This research was funded by GDR 2655 ‘Énergétique et adaptation des Hominidés’ and the ‘Louis Forest’ science grant awarded by the Chancellery of the Universities of Paris.

## References

- Abramoff MD, Magalhaes PJ, Ram SJ (2004) Image processing with ImageJ. *Biophoton Int* 11, 36–42.
- Beattie J (1927) The anatomy of the common marmoset (*Hapale jacchus* Kuhl.). *Proc Zool Soc London* 97, 593–718.
- Bishop A (1964) Use of the hand in lower primates. In: *Evolutionary and Genetic Biology of Primates*, Vol. 2 (ed. Buettner-Janusch J), pp. 133–225. New York: New York Academic.
- Carlson KJ, Patel BA (2006) Habitual use of the primate forelimb is reflected in the material properties of subchondral bone in the distal radius. *J Anat* 208, 659–670.
- Cartmill M, Milton K (1977) Lorisiform wrist joint and evolution of brachiating adaptations in Hominoidea. *Am J Phys Anthropol* 47, 249–272.



- Chatani K (2003) Positional behavior of free ranging Japanese macaques (*Macaca fuscata*). *Primates* **44**, 13–23.
- Erickson C (1957) The hands of the new world primates with comparative functional observations on the hands of other primates. *Am J Phys Anthropol* **15**(Suppl. 1), 446.
- Fleagle JG (1999) *Primate Adaptation and Evolution*. New York: Academic Press.
- Fleagle JG, Meldrum DJ (1988) Locomotor behavior and skeletal morphology of two sympatric pithecia monkeys, *Pithecia pithecia* and *Chiropotes satanas*. *Am J Primatol* **16**, 227–249.
- Fleagle JG, Mittermeier RA (1980) Locomotor behavior, body size, and comparative ecology of seven Surinam Monkeys. *Am J Phys Anthropol* **52**, 301–314.
- Garber PA (1991) A comparative study of positional behavior in three species of tamarin monkeys. *Primates* **32**, 219–230.
- Gautier-Hion A, Colyn M, Gautier JP (1999) *Histoire Naturelle des Primates d'Afrique Centrale*. Libreville: ECOFAC.
- Grand T (1968) Functional anatomy of upper limb. In: *Biology of the Howler Monkey* (ed. Malinow MR), pp. 104–125. New York: Karger.
- Hamrick MW (1996) Functional morphology of the lemuriform wrist joints and the relationship between wrist morphology and positional behavior in arboreal primates. *Am J Phys Anthropol* **99**, 319–344.
- Hill WCO (1957) *Primates Comparative Anatomy and Taxonomy, III, Pithecoide, Platyrrhini*. Edinburgh: Edinburgh University Press.
- Hill WCO (1959) The anatomy of *Callimico Goeldii* (Thomas), a primitive American primate. *Trans Am Phil Soc* **49**, 1–116.
- Hill WCO (1960) *Primates Comparative Anatomy and Taxonomy, IV, Cebidae, Part A*. Edinburgh: Edinburgh University Press.
- Hill WCO (1962) *Primates Comparative Anatomy and Taxonomy, V, Cebidae, Part B*. Edinburgh: Edinburgh University Press.
- Hill WCO (1966) *Primates Comparative Anatomy and Taxonomy, VI, Catarrhini*. Edinburgh: Edinburgh University Press.
- Hill WCO (1970) *Primates Comparative Anatomy and Taxonomy, VIII, Cynopithecinae (Papio, Mandrillus, Theropithecus)*. Edinburgh: Edinburgh University Press.
- Hill WCO (1974) *Primates Comparative Anatomy and Taxonomy, VIII, Cynopithecidae (Cercopithecus, Macaca, Cercopithecus)*. Edinburgh: Edinburgh University Press.
- Hunt KD, Cant JGH, Gebo DL, et al. (1996) Standardized descriptions of primate locomotor and postural modes. *Primates* **37**, 363–387.
- Jenkins FA (1981) Wrist rotation in primates: a critical adaptation for brachiators. *Symp Zool Soc London* **48**, 429–451.
- Jenkins FA, Fleagle JG (1975) Knuckle-walking and the functional anatomy of the wrists in living apes. In: *Primate Functional Morphology and Evolution* (ed. Tuttle RH), pp. 213–227. The Hague, Paris: Mouton.
- Jones RT (1967) The anatomical aspects of the baboon's wrist joint. *S Afr J Sci* **63**, 291–296.
- Jouffroy FK, Medina MF (2002) Radio-ulnar deviation of the primate carpus: an X-ray study. *Z Morph Anthropol* **83**, 275–289.
- Kingdon J (1988) Comparative morphology of hands and feet in guenons. In: *A Primate Radiation: Evolutionary Biology of the African Guenons* (eds Gautier-Hion A, Bourlière F, Gautier JP, Kingdon J), pp. 184–193. New York: Cambridge University Press.
- Kobayashi M, Garcia-Elias M, Nagy L, et al. (1997) Axial loading induces rotation of the proximal carpal row bones around unique screw-displacement axes. *J Biomech* **30**, 1163–1167.
- Lemelin P, Schmitt D (1998) The relation between hand morphology and quadrupedalism in primates. *Am J Phys Anthropol* **105**, 185–197.
- Lewis OJ (1965) Evolutionary change in the primate wrist and inferior radioulnar joints. *Anat Rec* **151**, 275–285.
- Lewis OJ (1969) The hominoid wrist joint. *Am J Phys Anthropol* **30**, 251–268.
- Lewis OJ (1971a) The contrasting morphology found in the wrist of semi-brachiating monkeys and brachiating apes. *Folia Primatol* **16**, 248–256.
- Lewis OJ (1971b) Brachiation and early evolution of Hominoidea. *Nature* **230**, 577–579.
- Lewis OJ (1974) The wrist articulations of the Anthroidea. In: *Primate Locomotion* (ed. Jenkins FJ), pp. 143–169. New York: Academic Press.
- Lewis OJ (1985) Derived morphology of the wrist articulations and theories of hominoid evolution. Part 1. The Lorisine joint. *J Anat* **140**, 447–460.
- Lewis OJ (1989) *Functional Morphology of the Evolving Hand and Foot*. Oxford: Clarendon Press.
- Moojen TM, Snel JG, Ritt MJPF, et al. (2002) Three-dimensional carpal kinematics *in vivo*. *Clin Biomech* **17**, 506–514.
- Moore DC, Crisco JJ, Trafton TG, et al. (2007) A digital database of wrist bone anatomy and carpal kinematics. *J Biomech* **40**, 2537–2542.
- Napier JR (1962) Fossil hand bones from the olduvai Gorge. *Nature* **196**, 409–411.
- Napier JR (1967) Evolutionary aspects of primate locomotion. *Am J Phys Anthropol* **27**, 333–341.
- Napier JR (1980) *Hands*. New York: Pantheon Books.
- Napier JR, Napier PH (1967) *A Handbook of Living Primates*. New York: Academic Press.
- Neu CP, Crisco JJ, Wolfe SW (2001) *In vivo* kinematic behaviour of the radio-capitate joint during wrist flexion-extension and radioulnar deviation. *J Biomech* **34**, 1429–1438.
- Ochsenbein I (2002) Etude de la main de Saimiri sciureus: approche anatomique et fonctionnelle. Ecole nationale vétérinaire de Lyon. Université Claude-Bernard, Lyon I (médecine-pharmacie).
- O'Connor BL (1975) The functional morphology of the cercopithecoid wrist and inferior radioulnar joints, and their bearing on some problems in the evolution of the Hominoidea. *Am J Phys Anthropol* **43**, 113–121.
- O'Connor BL, Rarey KE (1979) Normal amplitudes of radioulnar pronation and supination in several genera of anthropoid primates. *Am J Phys Anthropol* **51**, 39–43.
- Orr CM, Leventhal EL, Chivers SF, et al. (2010) Studying primate carpal kinematics in three dimensions using a computed-tomography-based markerless registration method. *Anat Rec* **293**, 692–709.
- Parsons FG (1900) The joints of mammals compared with those of Man: part II. *J Anat Physiol* **34**, 301–323.
- Patel BA (2009) Not so fast! – Speed effects on forelimb kinematics in cercopithecine monkeys and implications for digitigrade postures in primates. *Am J Phys Anthropol* **140**, 92–112.
- Patel BA (2010) The interplay between speed, kinetics, and hand postures during primate terrestrial locomotion. *Am J Phys Anthropol* **141**, 222–234.

- Patel BA, Carlson KJ** (2006) Bone density spatial patterns in the radius reflect habitual hand postures adopted by quadrupedal primates. *J Hum Evol* **52**, 130–141.
- Patel BA, Polk JD** (2010) Distal forelimb kinematics in *Erythrocebus patas* and *Papio anubis* during walking and galloping. *Int J Primatol*, **31**, 191–207.
- Patel BA, Wunderlich R** (2010) Dynamic pressure patterns in the hands of olive baboons (*Papio anubis*) during terrestrial locomotion: implications for cercopithecoid hand morphology. *Anat Rec* **293**, 710–718.
- Rawlins RG** (1993) Locomotive and manipulative use of the hand in the Cayo Santiago macaques (*Macaca mulatta*). In: *Hands of Primates* (eds Preuschoft H, Chivers DJ), pp. 21–30. Berlin: Springer.
- Richmond BG** (2006) Functional morphology of the midcarpal joint in knuckle-walkers and terrestrial quadrupeds. In: *Human Origins and Environmental Backgrounds* (eds Ishida H, Tuttle R, Pickford M, Ogiwara N, Nakatsukasa M), pp. 105–122. New York: Springer.
- Robertson DF** (1944) Anatomy of the South American woolly monkey (*Lagothrix*). Part I: the forelimb. *Zoologica (N.Y.)* **29**, 169–192.
- Rose MD** (1973) Quadrupedalism in primates. *Primates* **14**, 337–357.
- Rose MD** (1977) Positional behaviour of Olive baboons (*Papio anubis*) and its relationship to maintenance and social activities. *Primates* **18**, 59–116.
- Sarmiento EE** (1988) Anatomy of the hominoid wrist joint – its evolutionary and functional implications. *Int J Primatol* **9**, 281–345.
- Schmitt D** (1994) Forelimb mechanics as a function of substrate type during quadrupedalism in two anthropoid primates. *J Hum Evol* **26**, 441–457.
- Schmitt D, Hanna JB** (2004) Substrate alters forelimb to hindlimb peak force ratios in primates. *J Hum Evol* **46**, 239–254.
- Schreiber H** (1934) Zur Morphologie der Primatenhand I. Röntgenologische Untersuchungen an der Handwurzel der Affen. *Anat Anz* **78**, 369–456.
- Schwartz JH, Yamada TK** (1998) Carpal anatomy and primate relationships. *Anthropol Sci* **106**(Suppl.), 47–65.
- Sullivan WE** (1961) Skeleton and joints. In: *The Anatomy of the Rhesus Monkey* (eds Hartman CG, Straus WL), pp. 43–84. New York: Haffner Publishers.
- Tuttle RH** (1967) Knuckle-walking and the evolution of hominoid hands. *Am J Phys Anthropol* **26**, 171–206.
- Tuttle RH** (1969) Terrestrial trends in the hands of the Anthropoidea: a preliminary report. *Proc 2nd Int Con Primatol* **2**, 192–200. Basel: Karger.
- Whitehead PF** (1993) Aspects of the anthropoid wrist and hand. In: *Postcranial Adaptations in Nonhuman Primates* (ed. Gebo DL), pp. 96–120. Dekalb: Northern Illinois University Press.
- Yalden DW** (1972) Form and function of carpal bones in some arboreally adapted mammals. *Acta Anat* **82**, 383–406.
- Youlatos D** (1996) Atelines, apes and wrist joints. *Folia Primatol* **67**, 193–198.
- Youlatos D** (1999) The schizodactylous grasp of the howling monkey. *Z Morphol Anthropol* **82**, 187–198.
- Zieler LK** (1978) Functional morphology of forelimb joints in the woolly monkey *Lagothrix lagotricha*. *Contrib Primatol* **14**, 1–130. Basel: Karger.